Journal of Solid State Chemistry 184 (2011) 2629–2634

Contents lists available at ScienceDirect

Journal of Solid State Chemistry

journal homepage: www.elsevier.com/locate/jssc

$M^{II}Ge(PO_4)_2$ (M=Ca, Sr, Ba): Crystal structure, phase transitions and thermal expansion

Karin Popa [a], Gilles Wallez [b,*], Damien Bregiroux [b], Pascal Loiseau [b]

[a] "Al.I. Cuza" University, Department of Chemistry, 11-Carol I Blvd., 700506 Iasi, Romania
[b] Chimie ParisTech, UPMC Univ. Paris 06, CNRS-UMR 7574, Laboratoire de Chimie de la Matière Condensée de Paris (LCMCP), 75005 Paris, France

ARTICLE INFO

Article history:
Received 12 May 2011
Received in revised form
18 July 2011
Accepted 23 July 2011
Available online 30 July 2011

Keywords:
Phosphates
Crystal structure
Rietveld analysis
Phase transition
Thermal expansion

ABSTRACT

Three earth alkali-germanium monophosphates $M^{II}Ge(PO_4)_2$ (M=Ca, Sr, Ba) were prepared by solid state reaction and their structures, previously unknown, studied by Rietveld analysis. $BaGe(PO_4)_2$ and high-temperature β-$SrGe(PO_4)_2$ (space group $C2/m$, Z=2) are fully isotypic with yavapaiite, whereas $CaGe(PO_4)_2$ and low-temperature α-$SrGe(PO_4)_2$ ($C2/c$, Z=4) are distorted derivatives. The phase transition between the two forms is observed for the first time. The thermal expansion, resulting from several structural mechanisms, is very anisotropic.

1. Introduction

The $M^{II}M'^{IV}(PO_4)_2$ monophosphates (M=Cd, Ca, Sr, Pb, Ba; M'=Ge, Ti, Mo, Sn, Hf, Zr, Pu, Np, U, Th) have been studied during the last decades for their applications in the downstream of the nuclear cycle, either as host matrices for actinide radwastes or, more recently, as products of the reaction of the spent nuclear fuel with tributyl phosphate during the reprocessing [1–10]. They have also proved interesting as luminescent materials [11–13]. From a structural point of view, two main groups can be distinguished, depending on the coordination of the tetravalent cation:

the high-radius actinide occur in eight or ninefold coordination, like for cheralite-type compounds $CaAn(PO_4)_2$ in which Ca^{II} and An^{IV} occupy the same ninefold polyhedron [1–4]; if M^{II} and An^{IV} are different in size, the two cations adopt specific environments with different coordinations, as recently observed for $SrNp(PO_4)_2$ [9] and $BaAn(PO_4)_2$ (An=Th, Np) [10];
the M'^{IV} cations of the p- and d-block, in an octahedral coordination, form strong 2D $[M'^{IV}(PO_4)_2]^{2-}$ frameworks. Well-known members of this group are the phosphate isotypes of yavapaiite $KFe(SO_4)_2$ [14] (space group $C2/m$, Z=2), like $BaM'^{IV}(PO_4)_2$ (M'=Ge, Ti, Mo, Sn, Hf, Zr) [6,8,15–18], which will be termed "true yavapaiites" (TY) in the following. The yavapaiite structure consists in dense slabs of $M'^{IV}O_6$ octahedra and PO_4 tetrahedra, alternating along the c-axis with layers of M^{II} cations in tenfold coordination.

Several derivatives of this archetype, or "distorted yavapaiites" (DY) have been observed at room temperature for smaller M^{II} cations like in $SrTi(PO_4)_2$ and $SrSn(PO_4)_2$ (Z=4, $C2/c$) [18], $SrZr(PO_4)_2$ (Z=2, P-1) [17]. The $CaZr(PO_4)_2$ structure (Z=4, $P2_12_12_1$), the only one known for a calcium compound of this family, is clearly different from yavapaiite [19]; the coordinations of the cations are also different (7 for both Ca^{II} and Zr^{IV}). For $PbGe(PO_4)_2$, Apinitis et al. [20] proposed the Cc or $C2/c$ space group and similar cell parameters as those of $SrTi(PO_4)_2$, so this compound is probably another DY. On the opposite, $PbSn(PO_4)_2$ was found to have a very different 3D structure in which the $6s^2$ lone pair of Pb^{II} exhibits a strong stereochemical activity [21].

In this family, the $M^{II}Ge(PO_4)_2$ compounds are still widely unknown, except for their cell parameters and hypotheses on their space groups, of which some appeared dubious in our preliminary studies. No structural data is available. On the basis of their diffraction patterns, $BaGe(PO_4)_2$ [15,22], $SrGe(PO_4)_2$ [22] and $CaGe(PO_4)_2$ [23], obtained by solid state synthesis, were all reported as TY's, space group $C2/m$. Only $PbGe(PO_4)_2$ was grown as single crystals, at high temperature with flux [20]. The present study, first intended to propose a complete structural analysis of the ambient $M^{II}Ge(PO_4)_2$ forms (M=Ca, Sr, Ba), was extended to high temperatures in order to clear up the relationships between the different structural varieties in the yavapaiite family. At last, the study of their thermal expansion and their polymorphism is reported here for the first time.

* Corresponding author.
E-mail address: gilles.wallez@upmc.fr (G. Wallez).

0022-4596/$ - see front matter © 2011 Elsevier Inc. All rights reserved.
doi:10.1016/j.jssc.2011.07.037

2. Experimental

2.1. Synthesis

Stoichiometric amounts of $M^{II}CO_3$ ($CaCO_3$ 99.9%, Johnson Mattey; $SrCO_3$ 99%, Prolabo; $BaCO_3$ 98%, Aldrich), GeO_2 (99.98%, Alfa Aesar) and $NH_4H_2PO_4$ (98.5%, Sigma Aldrich) were mixed and heated in the first step for 12 h at 600 °C in an alumina crucible. The obtained powders were pressed into pellets and subjected to a new thermal treatment under air for 100 h at 1000 °C (M=Ca), 18 h at 1150 °C (M=Sr), and 72 h at 1100 °C (M=Ba), depending on the time needed to obtain a satisfactory purity when possible. From their diffraction patterns, the Ba^{II} and Sr^{II} samples appeared almost pure, but the temperature of 1100 °C found in the literature [15] proved insufficient for the synthesis of the latter. In contrast with the same previous work, which reports likewise a final annealing at 1050 °C for $CaGe_4(PO_4)_2$, we observed a decomposition of the intended product at this temperature. Indeed, the purest sample we obtained revealed the presence of $CaGe_4(PO_4)_2$ and $Ca_2P_2O_7$ with peak intensities reaching 4%.

2.2. Differential thermal analysis

Thermal stability and possible phase transitions were studied using a Setaram DTA-TG instrument. The powder samples, put into Pt crucibles, were heated and cooled under air at a 600 °C h^{-1} rate.

2.3. X ray powder diffraction

XRPD was performed on a Panalytical X'Pert Pro diffractometer with an incident-beam Ge monochromator, at U=45 kV and I=40 mA. The apparatus was equipped with an Anton Paar HTK 1200 N furnace for high temperature diffraction. The patterns for structural analysis were recorded over 12 h in the $10 \le 2\theta \le 140^\circ$ range (130° at high temperature), step 0.013°. For the measurement of the thermal expansion, the patterns were recorded at high temperature on a shorter $10 \le 2\theta \le 60^\circ$ range over 1 h. The Rietveld analyses were carried out with the Fullprof suite [24].

3. Results and discussion

3.1. $BaGe(PO_4)_2$

The barium compound has been reported several times as fully isotypic with yavapaiite [8,15]. The Rietveld analysis in Le Bail's (profile matching) mode confirmed its compatibility with the $C2/m$ space group. So, the atomic positions were refined starting from those of $KFe(SO_4)_2$ [14], with anisotropic thermal factors for Ba and Ge. Soft constraints were applied to the P–O distances. See Table 1 for further refinement parameters and crystallographic data. Reliability factors and cation–anion distances (Table 2) appeared satisfactory, thus allowing to confirm the $C2/m$ symmetry, which also

Table 1
Crystal data[a] and Rietveld refinement conditions.

Compound	$BaGe(PO_4)_2$	α-$SrGe(PO_4)_2$	β-$SrGe(PO_4)_2$	$CaGe(PO_4)_2$
Temperature (°C)	20	20	200	20
Space group	$C2/m$	$C2/c$	$C2/m$	$C2/c$
a (Å)	7.9672(2)	16.1787(8)	7.8695(5)	15.706(2)
b (Å)	5.0757(2)	5.0669(3)	5.0724(4)	5.0682(6)
c (Å)	7.7146(2)	7.8694(4)	7.3566(5)	7.7713(9)
β (deg.)	94.954(2)	115.087(3)	94.064(4)	117.029(6)
V (Å^3)/Z	310.80(2)/2	584.24(5)/4	292.92(3)/2	551.0(1)/4
2θ scan range/step (deg.)	9-140/0.013	9-140/0.013	9-130/0.013	9-140/0.013
Measured reflections	340	569	294	551
I-dependent/profile parameters	22/11	32/11	22/11	32/11
R_P	0.046	0.079	0.092	0.064
R_{WP}	0.071	0.11	0.13	0.10
R_{Bragg}	0.044	0.052	0.044	0.061
R_F	0.024	0.033	0.037	0.053
χ^2	10	28	19	19

[a] the *esd*'s given by the refinement program have been multiplied by 10

Table 2
Cation–anion distances (Å). Bond valence sums (*bvs*, v.u.) are calculated from Brese's bond valence parameters [26].

	$CaGe(PO_4)_2$		α-$SrGe(PO_4)_2$		β-$SrGe(PO_4)_2$		$BaGe(PO_4)_2$	
M	2 × O1	2.408(6)	2 × O1	2.667(4)	4 × O3	2.632(3)	4 × O3	2.810(2)
	2 × O2	2.571(5)	2 × O2	2.619(4)				
	2 × O4	2.405(3)	2 × O4	2.609(4)	2 × O2	2.599(4)	2 × O2	2.759(3)
	2 × O4	2.846(6)	2 × O4	2.781(5)	4 × O2	3.014(2)	4 × O2	3.024(2)
	2 × O4	3.236(6)	2 × O4	3.241(5)				
bvs		*1.86*		*1.93*		*1.90*		*2.09*
Ge	2 × O1	1.875(5)	2 × O1	1.877(4)	4 × O3	1.893(3)	4 × O3	1.866(2)
	2 × O2	1.891(5)	2 × O2	1.873(4)				
	2 × O3	1.827(4)	2 × O3	1.847(4)	2 × O1	1.834(4)	2 × O1	1.848(3)
bvs		*4.40*		*4.36*		*4.29*		*4.43*
P	O1	1.548(6)	O1	1.561(4)	2 × O3	1.557(3)	2 × O3	1.555(2)
	O2	1.553(6)	O2	1.569(4)				
	O3	1.518(4)	O3	1.521(4)	O1	1.522(4)	O1	1.515(3)
	O4	1.514(2)	O4	1.516(3)	O2	1.511(4)	O2	1.541(3)
bvs		*4.85*		*4.74*		*4.80*		*4.74*

O1 (β form) corresponds to O3 (α),O2 (β) to O4 (α); O3 (β) splits into O1 (α) and O2 (α)

prevails for the other Ba$M'^{IV}(PO_4)_2$ compounds [6,15–18]. An endothermal accident observed at 1161 °C (1130 °C on cooling) by DTA may correspond to a transition to the rhombohedral (*P*-3*m*1) form observed for $BaZr(PO_4)_2$ [8], but this temperature was exceedingly high for XRPD measurements. Melting occurs at 1234 °C.

Note that the aforementioned Ba*An*$(PO_4)_2$ compounds – also layered structures – crystallize in the same space group as $BaGe(PO_4)_2$, with cations occupying the same special positions, but with higher coordination numbers (14 for Ba, 8 for *An*) in agreement with their higher radii [10].

3.2. α-*SrGe(PO₄)₂*

An attempt to refine the diffraction pattern of the strontium compound recorded at room temperature with the previous structural model yielded anomalous high reliability factors and intensity residuals. Several small peaks also remained unindexed, which appeared as the $h+l=2n+1$ superstructure reflections of a *C*2/*c* doubled cell similar to that determined by Zhao et al. [18] for $SrTi(PO_4)_2$. This result contradicts three studies of the 1970s and early 1980s which concluded in the *C*2/*m* symmetry, without solving the structure, however [15,22,23]. The refinement of the structure, termed α-$SrGe(PO_4)_2$ in the following, was carried out in the same conditions as the previous one, resulting in the final Rietveld plot shown in Fig. 1. The crystal structure is drawn in Fig. 2.

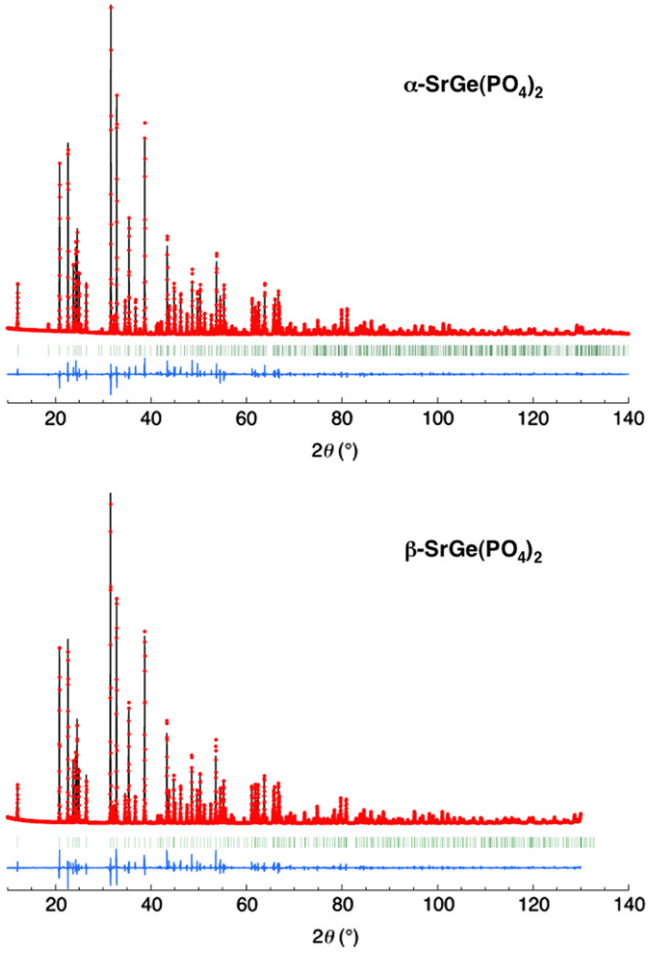

Fig. 1. Rietveld plots for α-$SrGe(PO_4)_2$ and β-$SrGe(PO_4)_2$: y_{obs} (dots), y_{calc} (solid, upper), $y_{obs}-y_{calc}$ (solid, lower), Bragg positions (bars).

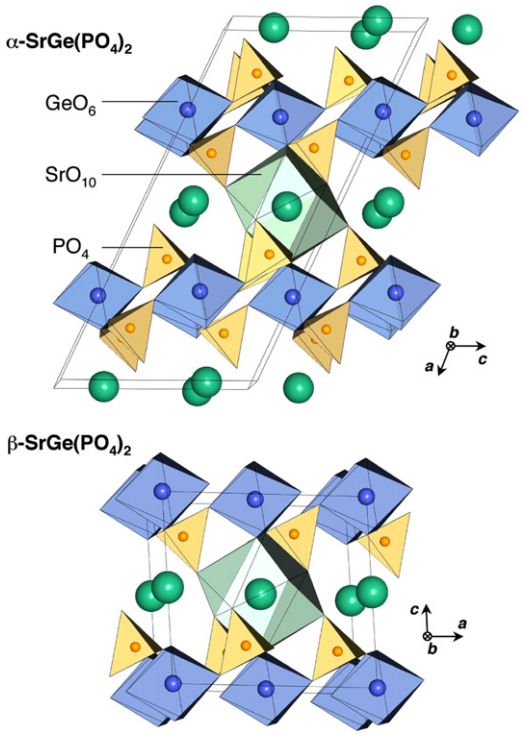

Fig. 2. Tilted (0 1 0) projections of the crystal structures of α-$SrGe(PO_4)_2$ (top) and β-$SrGe(PO_4)_2$ (bottom). For clarity, only the central SrO_{10} polyhedron has been drawn.

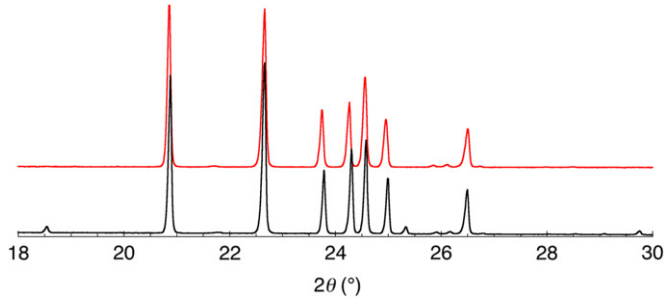

Fig. 3. Diffraction patterns of α-$SrGe(PO_4)_2$ (20 °C, lower plot) and β-$SrGe(PO_4)_2$ (200 °C, upper plot). Note the extinction of the peaks with $h+l=2n+1$ (underscored) in the high-temperature form.

3.3. *β-SrGe(PO₄)₂*

Around 195 °C, the typical diffraction peaks of the *C*2/*c* superstructure vanish (Fig. 3), which can be considered as a signature of a phase transition to the *C*2/*m* TY form. A faint break in the slope of the DTA curve was observed at this temperature. The cell edges of the double-cell DY correspond to those of the TY by the following vectorial relations, in agreement with the extinction rule observed:

$$\boldsymbol{a}_{DY}=-\boldsymbol{a}_{TY}-2\boldsymbol{c}_{TY} \quad \boldsymbol{b}_{DY}=\boldsymbol{b}_{TY} \quad \boldsymbol{c}_{DY}=\boldsymbol{a}_{TY}$$
$$\boldsymbol{a}_{TY}=\boldsymbol{c}_{DY} \quad \boldsymbol{b}_{TY}=\boldsymbol{b}_{DY} \quad \boldsymbol{c}_{TY}=(\boldsymbol{a}_{DY}+\boldsymbol{c}_{DY})/2$$

The crystal structure of this high temperature (β) form (Fig. 2) was refined from a diffraction pattern recorded at 200 °C. A careful comparison of the α and β forms of $SrGe(PO_4)_2$ allows to discuss the evolution of the geometry of the coordination polyhedra and the mechanism of the phase transition:

because of the high covalency of the P–O and Ge–O bonds, the PO_4 tetrahedron and the GeO_6 octahedron only sustain minor

distortions; indeed, the whole $[Ge(PO_4)_2]^{2-}$ framework remains nearly unchanged;
in the β form, the SrO_{10} polyhedron, which consists in six close oxygens forming an elongated octahedron (<2.64 Å) capped by four external O2's at 3.01 Å, obeys to a $2/m$ symmetry. At low temperature, the mirror is lost by a strong shift of Sr^{II} along the *b*-axis towards two of the external oxygens (termed O4 in the β form), thus reducing the distance to 2.78 Å (-0.23 Å) and increasing the distance of the two other forms to 3.24 Å ($+0.23$ Å). For a similar array in the $SrTi(PO_4)_2$ and $SrSn(PO_4)_2$ DY forms, Zhao et al. proposed an eightfold coordination for Sr^{II} [18], but considering the solid angle still occupied by the two outmost oxygens, we take them into account and propose an "8+2" coordination, a more suitable environment for Sr^{II} than the true tenfold polyhedron in the TY form.

Conceivably, the kinship of the two structural forms, $SrTi(PO_4)_2$, $SrSn(PO_4)_2$ and $PbGe(PO_4)_2$ (DY) should allow a similar α–β transition at high temperature; likewise the $BaM'^{IV}(PO_4)_2$ TY's may distort below room temperature.

3.4. $CaGe(PO_4)_2$

As seen before, our $CaGe(PO_4)_2$ sample contained non-negligible amounts of $CaGe_4(PO_4)_2$ and $Ca_2P_2O_7$, which had to be treated as secondary phases (with fixed atomic coordinates) in the Rietveld analysis. The structural data for $CaGe_4(PO_4)_2$, which were not found in the literature, were inferred from those of $NaZr_2(PO_4)_3$ [25], owing to the obvious isotypy of the spurious phase with the well-known NZP (Nasicon) model. In the absence of superstructure peaks, and in agreement with Keller's ICDD file [23] the structure was first considered as a $C2/m$ TY and refined starting from the data set of β-$SrGe(PO_4)_2$. The results were rather poor, with exceedingly high reliability factors ($R_{Bragg} \approx 0.08$) and thermal parameter for Ca ($B_{iso} \approx 3$), leading us to consider the $C2/c$ DY structure instead. This model proved more satisfactory, and the final position of Ca ($y=0.7928(5)$) appeared much closer to that of Sr (0.7867(2)) than to the central position (0.75). The calculated intensities for the superstructure peaks are actually very low; considering that the DY modification consists mostly in a shift of the earth-alkali cation, this difference with the XRD pattern of the Sr compound results simply from the lower atomic number of Ca.

As mentioned before, even a prolonged annealing did not allow to obtain pure $CaGe(PO_4)_2$. Similar attempts were made by us to synthesize unreported $CaTi(PO_4)_2$ but the solid state reaction even failed totally. At this point, it is noteworthy to emphasize on the scarcity of the literature dealing with the $CaM'^{IV}(PO_4)_2$ (M'=Ge, Ti, Mo, Sn, Hf, Zr) monophosphates in general, compared to their Sr and Ba analogs. Yet, the Ca^{II} compounds are generally more studied and better known than the latters, but to this date, besides the brief aforementioned studies on $CaGe(PO_4)_2$, only $CaZr(PO_4)_2$ has sustained a detailed structural analysis [19], which has revealed a non-yavapaiite framework ($P2_12_12_1$) and Ca^{II} surrounded by seven oxygens only. So far, two explanations can be proposed:

the "8+2" coordination in the $C2/c$ DY structure, convenient for Sr^{II}, is too high for Ca^{II}, which makes this form poorly stable;
on the opposite, Ca^{II} finds a sixfold coordination in the NZP-like $CaGe_4(PO_4)_6$ unwanted phase. This structure is known to be a very stable host matrix for Na^{I}-size cations like Ca^{II}, but less adapted to bigger ones like Sr^{II} and Ba^{II}. The absence of data concerning would-be magnesium derivatives that could be explained likewise.

3.5. Thermal expansion

The thermal expansion of the three compounds has been investigated by high temperature XRD. For convenience, all the coefficients of thermal expansion (CTE, or α in the $\Delta l/l_o=\alpha.\Delta T$, calculated by linear regression) will be expressed following the crystallographic axes of the $C2/m$ TY form (Table 3). The structural mechanisms are shown in Fig. 4.

The high CTE of the *c*-axis in all the $MGe(PO_4)_2$ forms results from the weakness of the M^{II}–O bonds in the interslabs. Actually, such a strong expansion of the stacking axis is very common among the layered structures. In the present case, it is increased by the Coulombic repulsions between edge-sharing cations M^{II} and Ge^{IV} (Fig. 4, M1). A similar behavior was observed in $BaZr(PO_4)_2$ [8].

The case of the *b*-axis is very different. In this direction, the cohesion of the slabs is due to infinite chains of corner-connected GeO_6 and PO_4 polyhedra, which makes the cell parameter correspond to the total length of their two *b*-directed O–O edges. Therefore, *b* does not change significantly with the crystalline form and the radius of the M^{II} cation (Table 1). Neither can it be affected by the expansion of the M^{II}–O bonds, on the opposite to the other cell edges, nor the GeO and PO bonds are strong enough to remain nearly unaffected by the heating. So α_b will be determined mostly by the orientation of these edges and dynamic effects:

in DY's, the O–O edges form slight zig-zags (170.3(7)° in α-$SrGe(PO_4)_2$ at 20 °C), but the thermal evolution to the TY form makes them tend to the strict parallelism imposed by the *m*-mirror (Fig. 4, M2), thus resulting in a moderate α_b.

Table 3
Coefficients of thermal expansion (10^{-6} °C^{-1}) measured along the crystallographic axes of the $C2/m$ TY form.

Form	$CaGe(PO_4)_2$	α-$SrGe(PO_4)_2$	β-$SrGe(PO_4)_2$	$BaGe(PO_4)_2$
Structural type	$C2/c$ DY	$C2/c$ DY	$C2/m$ TY	$C2/m$ TY
α_a	10.7	0.4[a]	15.8	13.7
α_a	6.0	8.3	2.0	1.8
α_a	18.2	11.2	15.1	17.9
$\alpha_a=\alpha_v/3$	11.6	6.6[a]	11.0	11.1

[a] unprecise values due to narrow domain and non-linear variations.

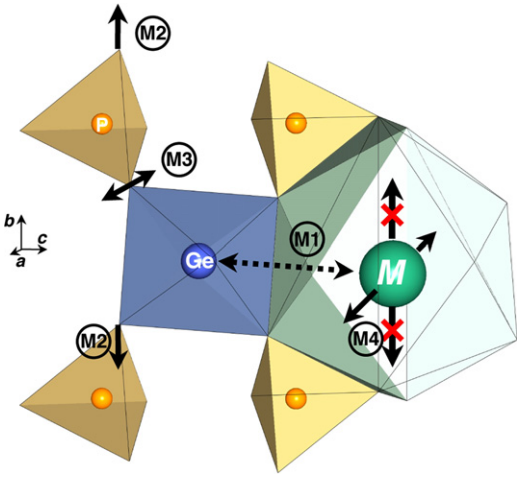

Fig. 4. Mechanisms of thermal expansion in the $MGe(PO_4)_2$ (M=Ca, Sr, Ba): Coulombic repulsion between M^{II} and Ge^{IV} (M1); alignment of the O-O edges following *b* (DY form, M2); transverse rocking of the oxygen (TY form, M3); expansion of the MO_{10} polyhedron contained following *b* (M4). Axes of the $C2/m$ form.

$CaGe(PO_4)_2$ also obeys to this model even if the DY–TY transition is too high to be observed, or simply does not occur. the origin of the remarkable low α_b values for TY's is probably to be found in the classical rocking effect observed in arrays corner-connected polyhedra (Fig. 4, M3) [27], even if the expansion remains positive due to the presence of the M^{II} cation.

The expansion along the *a*-axis means the stretching of the $[Ge(PO_4)_2]^{2-}$ slabs, allowed by their folded structure and their ability to adapt to important variations of the M^{II} radius (for example, *a* increases by 0.1 Å when Ba^{II} is substituted for Sr^{II} in the TY form (Table 1)). A possible explanation for the high values of α_a in the TY forms is based on a coupling effect (Fig. 4, M4): as seen before, the expansion of the Ca–O bonds along the *b*-axis is blocked by the tension of the GeO_6–PO_4 chains, resulting in a stronger expansion following *a*. On the contrary, the DY structure of $CaGe(PO_4)_2$, which allows an expansion along *b* only sustains a moderate expansion following *a*. Similar coupled effects in "networks with bond thermal expansion" have been described by Sleight [27].

The differences between the thermal behaviors of the DY and TY forms are highlighted by the breaks at the transition point in the expansion plots for $SrGe(PO_4)_2$ (Fig. 5).

Furthermore, the β angles of the two forms show opposite variations with temperature (Fig. 6). Conceivably, the negative slope in the TY domains could correspond to an evolution towards an orthogonal lattice compatible with the high-temperature trigonal form. The origin of the positive slope in the DY domains is not clear to us, but at least, the similar evolution of α-$SrGe(PO_4)_2$ and $CaGe(PO_4)_2$ is another evidence of the DY nature of the latter.

3.6. Polymorphism

Both the *C*2/*c*–*C*2/*m* and the *C*2/*m*–*P*-3*m*1 phase transitions observed in this family of compounds appear as displacive phenomena. However, in agreement with DTA, the former is clearly a second order one, that results from a continuous shift of the M^{II} cation towards the center of the oxygen polyhedron, whereas the latter is a first order one, which involves a modification of the $[Ge(PO_4)_2]^{2-}$ framework, as seen with $BaZr(PO_4)_2$ [8]. We can now propose a global scheme for the thermal evolution of the different yavapaiite forms (Fig. 7). The increase of the coordination number of the earth-alkali cation with temperature is somewhat uncommon, but it finds an explanation in the increase of the symmetry.

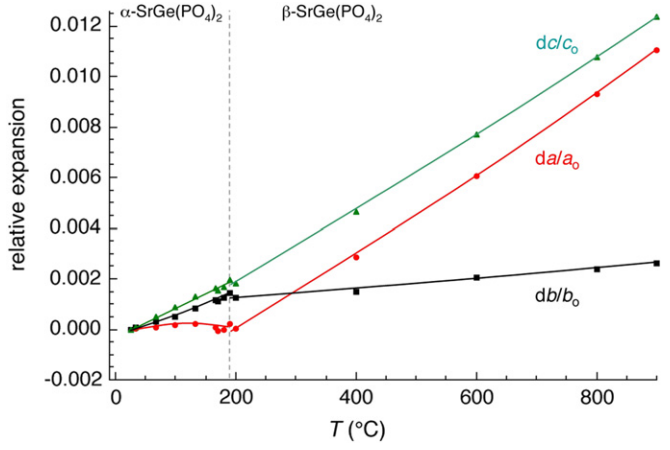

Fig. 5. Relative variation with temperature of the cell edges of $SrGe(PO_4)_2$ (*C*2/*m* TY setting for both forms). *esd*'s are estimated at 10^{-4}.

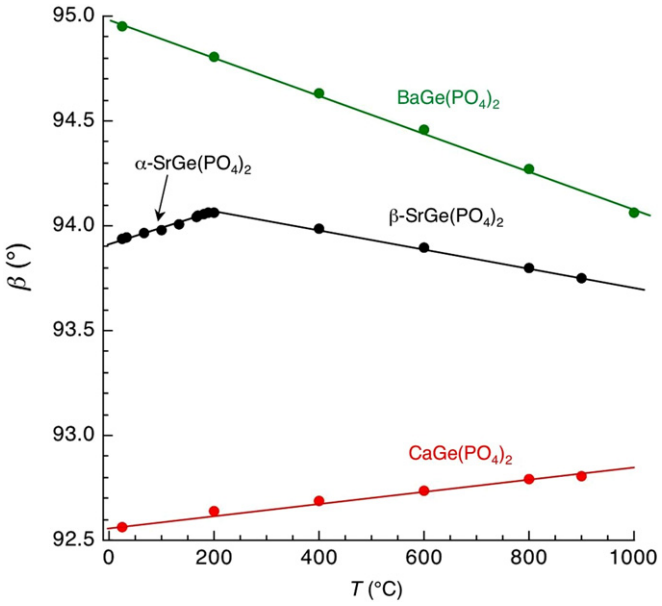

Fig. 6. Thermal evolution of the β angles (*C*2/*m* setting) of the $M^{II}Ge(PO_4)_2$ (M=Ca, Sr, Ba). Note the positive slopes for the *C*2/*c* forms and the negative slopes for the *C*2/*m* ones. *esd*'s are estimated at 0.02°.

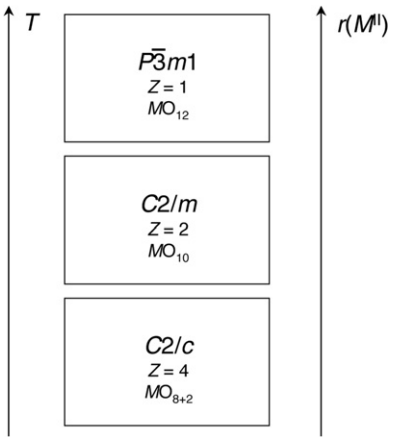

Fig. 7. A model of thermal evolution for the structures of the yavapaiite family.

4. Conclusion

In agreement with the previous works, $BaGe(PO_4)_2$ adopts the same typical yavapaiite structure as its Ti, Mo, Sn, Hf and Zr homologs. However, the shift of the smaller M^{II} cations towards the edge of the polyhedron and the subsequent distortion of the $CaGe(PO_4)_2$ and $SrGe(PO_4)_2$ structures contradict the literature. This environment, still too wide for Ca^{II}, explains the poor stability of $CaGe(PO_4)_2$, an argument which can be probably extended to the other existing or would-be $CaM'^{IV}(PO_4)_2$ with yavapaiite structure. So these Ca^{II} compounds appear of limited interest as materials, and their occurrence in the products of the nuclear fuel reprocessing is improbable.

On the contrary, the $[Ge(PO_4)_2]^{2-}$ framework, thanks to its polymorphism, appears well adapted to bigger Ca^{II} and Sr^{II} cations. The so-formed compounds, more stable, might be used for their optical and electrical properties. For instance, our recent study reveals that $SrGe(PO_4)_2$ and $BaGe(PO_4)_2$ show excellent dielectric performances at high frequency, making them promising materials for use in microwave applications [28].

Besides, the yavapaiite monophosphates appear as an interesting field for the study of the thermal mechanisms responsible for their complex expansion and their polymorphism. Further studies on the other forms of DY's could evidence similar phase transitions.

Supporting information available

Further details of the crystal structure investigations may be obtained from Fachinformationzentrum Karlsruhe, 76344 Eggenstein-Leopoldshafen, Germany (fax: (+49)7247–808-666; e-mail: crystaldata@fiz-karlsruhe.de, http://www.fiz-karlsruhe.de/request_for_deposited_data.html) on quoting CSD number 423040 ($BaGe(PO_4)_2$), 423041 (α-$SrGe(PO_4)_2$), 423042 (β-$SrGe(PO_4)_2$), and 423043 ($CaGe(PO_4)_2$).

Acknowledgments

K.P. acknowledges La Mairie de Paris for the "Research in Paris" 2010–2011 fellowship.

Appendix A. Supplementary information

Supplementary data associated with this article can be found in the online version at doi:10.1016/j.jssc.2011.07.037.

References

[1] D. Rose, Neues Jahrb. Mineral. Monatsh. 247 (1980) 247.
[2] A. Tabuteau, M. Pagès, J. Livet, C. Musikas, J. Mater. Sci. Lett. 7 (1988) 1315.
[3] J.M. Montel, J.L. Devidal, D. Avignant, Chem. Geol. 191 (2002) 89.
[4] V. Brandel, N. Dacheux, J. Solid State Chem. 177 (2004) 4755.
[5] D. Bregiroux, R. Belin, R. Valenza, F. Audubert, D. Bernache-Assollant, J. Nucl. Mater. 336 (2007) 52.
[6] K. Popa, D. Bregiroux, R.J.M. Koenings, T. Gouder, A.F. Popa, T. Geisler, P.E. Raison, J. Solid State Chem. 180 (2007) 4346.
[7] P.E. Raison, R. Jardin, D. Bouëxière, R.J.M. Konings, T. Geisler, C.C. Pavel, J. Rebizant, K. Popa, Phys. Chem. Minerals 35 (2008) 603.
[8] D. Bregiroux, K. Popa, R. Jardin, P.E. Raison, G. Wallez, M. Quarton, M. Brunelli, C. Ferrero, R. Caciuffo, J. Solid State Chem. 182 (2009) 1115.
[9] G. Wallez, D. Bregiroux, K. Popa, P.E. Raison, C. Apostolidis, P. Lindqvist-Reis, R.J.M. Konings, A.F. Popa, Eur. J. Inorg. Chem. (2011) 110.
[10] K. Popa, G. Wallez, P.E. Raison, D. Bregiroux, C. Apostolidis, P. Lindqvist-Reis, R.J.M. Konings, Inorg. Chem. 49 (2010) 6904.
[11] G. Blasse, G.J. Dirksen, Chem. Phys. Lett. 62 (1979) 19.
[12] C.R. Miao, C.C. Torardi, J. Solid State Chem. 155 (2000) 229.
[13] Z.J. Zhang, J.L. Yuan, X.J. Wang, D.B. Xiong, H.H. Chen, J.T. Zhao, Y.B. Fu, Z.M. Qi, G.B. Zhang, C.S. Shi, J. Phys. D: Appl. Phys. 40 (2007) 1910.
[14] E.J. Graeber, A. Rosenzweig, Am. Mineral. 56 (1971) 1917.
[15] R. Masse, A. Durif, C. R. Acad. Sci. Paris C 274 (1972) 1692.
[16] A. Leclaire, M.M. Borel, J. Chardon, B. Raveau, J. Solid State Chem. 116 (1995) 364.
[17] K. Fukuda, T. Iwata, A. Moriyama, S. Hashimoto, J. Solid State Chem. 179 (2006) 3870.
[18] D. Zhao, H. Zhang, Z. Xie, W.L. Zhang, S.L. Yang, W.D. Cheng, Dalton Trans. (2009) 5310.
[19] K. Fukuda, K. Fukutani, Powder Diffr. 18 (2003) 296.
[20] S. Apinitis, U. Sedmalis, P.R.S. Latv., Zinat. Akad. Vestis Kim. Ser. 6 (1984) 643.
[21] E. Morin, G. Wallez, S. Jaulmes, J.C. Couturier, M. Quarton, J. Solid State Chem. 136 (1998) 283.
[22] M.T. Paques-Ledent, J. Inorg. Nucl. Chem. 39 (1977) 11.
[23] L.P. Keller, G.J. McCarthy, I.C.D.D. Grant-in-Aid, JCPDS File no. 33-150, North Dakota State University, Fargo, North Dakota, USA, 1982.
[24] J. Rodriguez-Carvajal, FULLPROF.2k: Rietveld, profile matching and integrated intensity refinement of X-ray and neutron data, V 1.9c, Laboratoire Léon Brillouin, CEA, Saclay, France, 2001.
[25] L.O. Hagman, P. Kierkegaard, Acta Chem. Scand. 22 (1968) 1822.
[26] N.E. Brese, M. O'Keeffe, Acta Cryst. B 47 (1991) 192.
[27] A.W. Sleight, Inorg. Chem. 37 (1998) 2854.
[28] F. Tudorache, K. Popa, L. Mitoseriu, N. Lupu, D. Bregiroux, G. Wallez, J. Alloys Compd., in press, doi:10.1016/j.jallcom.2011.06.072.